Failure analysis of a jaw in a universal testing machine used for material strength testing

Edwin Espinel Blanco
Faculty of Engineering
Francisco de Paula Santander University Ocaña, Colombia
eeespinelb@ufpso.edu.co

Eder Norberto Florez Solano
Faculty of Engineering
Francisco de Paula Santander University Ocaña, Colombia
enflorezs@ufpso.edu.co

NarenYesith Pérez Rangel
Faculty of Engineering
Francisco de Paula Santander University Ocaña, Colombia
nyperezr@ufpso.edu.co

Abstract- A methodology is proposed to perform failure analysis on materials organized in three stages: (1) visual inspection of the failure, (2) material characterization tests, and (3) finite element analysis. The fracture presented in one of the jaws of a universal testing machine used for material strength testing was analyzed. Visual inspection revealed the type of failure corresponding to a brittle material, and Arc/Spark Optical Emission Spectrometry revealed the composition of the material. The metallography showed the formation of martensite typical of medium-carbon steels subjected to quenching heat treatment. Scanning electron microscopy showed the precipitation of carbides at the grain boundary, as well as the presence of voids and other metallic and non-metallic inclusions in the microstructure. With the simulation carried out by finite element analysis, it was observed that the part is subjected to fatigue loading. The methodology proposed allowed finding the cause of failure and proposing a solution by identifying possible hidden failures to solve the root of the problem.

Keywords – Failure Analysis, Fracture, Visual Inspection, Characterization, Fatigue

I. INTRODUCTION

The main objectives of maintenance are to provide reliable and safe operation of equipment and machines at all times, reduce costs, minimize downtime, and have comprehensive planning and execution of work to ensure operation [1].To achieve this objective, the functions and possible functional failures should be clearly defined, that is to say, the inability of an equipment to fulfill its function, in order to adopt a policy for the management there of [2]. Reliability engineering and predictive maintenance have two main objectives. Firstly, prevent catastrophic failures of critical production systems in a plant. Secondly, avoid deviations from acceptable performance levels that result in physical injuries, environmental impact, loss of capacity, or poor product quality [3].

One of the tools used for this purpose is failure analysis, defined as the process of making observations and collecting analytical data to determine how a component failed, and then applying engineering principles to define why the failure occurred and what should be done in order to prevent future failures [4-5]. In failure analysis are involved branches of engineering as varied as material science, manufacturing processes, thermodynamics and heat transfer, among others [6]. As a result, this analysis is used in the solution of different engineering problems, to mention just a few: failure of diesel-engine crankshafts [7], analysis of natural gas pipeline [8], and it is even applicable to smaller elements such as steel cables.

When performing a failure analysis, the Equipment Maintenance Log Sheet, maintenance plants, failure rate record of the machine, the data sheet, to know the conditions under which the failure occurred and so forth, should be taken into account. The more data and elements are available, the more accurate is the analysis [9]. The availability of satisfactory methods for the evaluation of equipment that fails unexpectedly is of paramount importance. Failure

studies provide valuable information to meet future design needs [10]. Metallurgical failure analysis can be defined as the process by which the mechanisms responsible for the failure of metal components are determined [11].

This work presents the identification of the root cause of a fracture failure in one of the jaws in a universal testing machine used to perform material strength testing in the mechanical engineering laboratory of Francisco de Paula Santander University in the municipality of Ocaña, Colombia. The strength of materials laboratory of Francisco de Paula Santander University located in the municipality of Ocaña, Norte de Santander Department in Colombia, has a universal testing machine model PU-300M manufactured by the company Pinzuar Ltda, to perform mechanical strength tests on materials. One of the pieces that make up the jaws system presented a fracture in the upper part. This piece allows the operator to open or close the jaws to introduce or extract the sample. It is not known what caused the failure of the piece since the machine is mainly used for teaching and scientific research. As a result, the machine is not constantly subjected to high loads that could have generated mechanical fatigue failure.

The failure in the piece that composes the jaws system of the PU-300M universal testing machine prevents the sample from being secured in the correct way for the test, preventing the tests from being carried out. The problem associated with this failure is that this element is not considered susceptible to this type of failure. Therefore, its appearance caused the complete stop of the equipment. Additionally, the manufacturer does not have this part in stock. As a result, it is not available for purchase by the user. The failure generated the need to perform a root cause analysis to determine the cause of failure, as well as the material required for manufacturing the part so that the machine can be put back into operation.

II. Materials and Methods

This work was carried out following the methodology proposed in Figure 1, which is based on failure analysis. The methodology consists of three stages. Firstly, a description of the failure was developed through visual inspection. This was done by analyzing the operating conditions of the machine, taking measurements and pictures, and inspecting the part. Subsequently, the type of failure was compared with theoretical studies. Secondly, the characterization of the part was carried out using hardnes stests, metallography, Arc/Spark Optical Emission Spectrometry, and scanning electron microscopy (SEM) with energy-dispersive X-ray spectrometry (EDS).

Thirdly, the part was modeled and simulated using finite element analysis (FEA). Solidworks was used to draw the part, and Ansys was used to simulate the mechanical behavior of the element when subjected to loads during operation. Finally, the methodology proposed in the characterization stage, based on the analyses carried out in the three stages, allows the identification of the root cause of the failure and the evaluation of a solution to avoid future failures and, if possible, to solve potential hidden failures found during the characterization process.

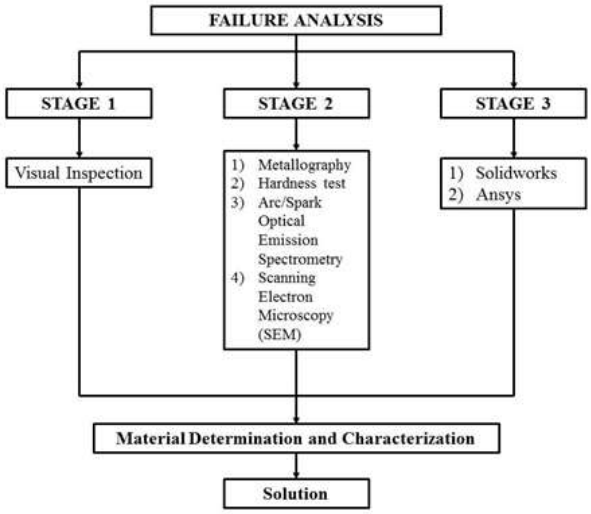

Figure 1. Methodology proposed for the failure analysis.

2.1 Visual inspection–

This stage allowed understanding the operation of the universal testing machine used to carry out tensile and compression tests on materials. Figure 2a shows the Universal Testing Machine model PU-300M manufactured by Pinzuar Ltda. This machine is used to perform tensile, compression, and bending tests on different metallic and non-metallic materials to determine their maximum stress and deformation coefficients. The jaws system (figure 2 b, c) is responsible for holding the sample during the tensile test. The force vs. time data is recorded in a software. This software provides the deformation graph of the material, as well as the maximum load the material can withstand. The test ends when the sample breaks.

a) b) c)

Figure 2. a) Universal Testing Machine, b) Upper jaw, and c) Lower jaw

During the tensile test on a standardized steel sample, one of the parts of the jaws system presented a fracture in its upper part. This part allows the operator to open or close the jaws to introduce or extract the sample. It is not known what caused the failure of the part. As a result, measurements and pictures of the part were taken. Then, a comparative analysis was made, based on the types of failures found in the literature review [12].

2.2. Destructive testing –

The piece was physically and chemically characterized. Arc/spark optical emission spectrometry tests were carried out to determine the percentage of each chemical element that makes up the piece. Also, metallography analysis and hardness tests were performed to observe the surface microstructure and the hardness of the material to deformation. Finally, scanning electron microscopy (SEM) with energy-dispersive X-ray spectrometry (EDS) was used to observe the microstructure and morphology of the material. The data obtained was analyzed to determine the cause of failure [13].

Hardness tests and spectrometry results can be used to determine the material from which the part was originally manufactured [14]. Metallography and scanning electron microscopy (SEM) can be used to determine whether the material was subjected to any heat treatment to change its properties [15]. Based on the analysis of the results obtained, possible design or manufacturing errors can be detailed, which can be critical points in the appearance of the failure [16].

To carry out the tests, 1cm x 1cm x 1cm samples were selected from the material under study. For the metallography, the surface of the test sample was polished to a mirror-like appearance. Then, the surface was chemically etched in Nital and Kalling solutions. For the SEM, the sample was gold-coated to obtain better conductivity and, therefore, better micrographs. This allowed detailing what happened to the material, as well as determining if the material was subjected to heat treatments after its manufacture.

The metallographic analysis was carried out with an Optikamicroscope, model B-157ALC, following the specifications of the ASTM E3 - 11 standard. The sample was prepared in Bakelite for its later polishing. Then, it was sanded and polished until it acquired a mirror-like appearance. Finally, it was etched with a solution of Nital and Picral. Each sample was observed at 50X, 100X, 200X, and 400X magnifications. The hardness test was carried out in a Mitutoyo HR-300 hardness tester, under the guidelines of ASTM E18-19 standard. 10 hardness values were taken at different points of the piece. Figure 3 shows the sample with the points where the hardness measurements were taken. The chemical composition analysis of the sample was carried out using a Bruker Q4 TASMAN spectrometer. The SEM images were obtained using a piece of equipment JCM-6000PLUS.

Figure 3. Sample with hardness test points.

2.3. Finite Element Analysis –

The piece under study was modeled using SolidWork CAD software. Then, the behavior of the part was simulated by applying the loads for working conditions using Ansys software. Figure 4 shows the solid of the part modeled in SolidWork.

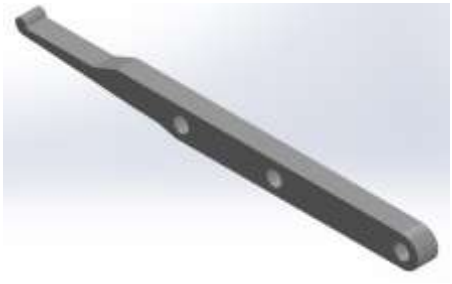

Figure 4. Solid of the piece modeled in solidworks.

Static and dynamic analyses of the piece were carried out to highlight possible critical points, to better understand the causes of failure in the material. The finite element analysis is intended to understand the behavior of the material when subjected to stress during the operation of the machine. This allows proposing a solution that mitigates the failure and avoids further damage to the machine or possible accidents involving operator safety.

III. Results and Discussion

3.1. Visual inspection –

Figure 5 shows the part where the failure occurred. The part was visually inspected and measured. A photographic report was prepared to make a comparison that allowed the classification of the type of failure presented. Toughness is the term used to define a material's ability to plastically deform and absorb energy. Terms such as ductile or brittle are commonly used to define high-toughness (ductile) or low-toughness (brittle) materials. In this context, cleavage fracture is the most brittle fracture mechanism that can originate in crystalline materials. Cleavage fracture can be defined as an extraordinarily rapid propagation of a crack, by the simple separation of the atomic bonds, along a given crystallographic plane [17].

Figure 5. Failure of the clamping piece of the jaw.

The visual inspection seeks to detail the physical nature of the object inspected. Among these are the size, shape, surface texture, and condition in which it is found, as well as the detail of the defects that allow an assessment of the state in which the material under study is found [18]. Figure 6 shows a fracture of the piece without plastic deformation with a granular appearance on the surface generated by normal stress applied at approximately 90° in the direction of the load. This leads to contemplating the hypothesis of brittle fracture [19].

Figure 6. Fracture in the clamping piece of the jaw.

3.2. Destructive Testing –

Table 1 shows the hardness test results of the sample. The material has a uniform hardness with an average value of 20.86 Rockwell C. Table 2 shows the spectroscopy test results for each of the elements that make up the sample with their respective percentages.

Table -1 Sample Hardness Test

Rockwell C Hardness										
P 1	**P 2**	**P 3**	**P 4**	**P 5**	**P 6**	**P 7**	**P 8**	**P 9**	**P 10**	**Ø**
21.20	20.60	21.20	21.10	20.60	20.60	21.30	20.10	21.00	20.90	**20.86**

Ø:Average
P: Test point.

Table -2 Chemical composition of the sample, Arc/spark optical emission spectrometry results

Arc/spark optical emission spectrometry results										
	C %	**Si %**	**Mn %**	**P %**	**S %**	**Cr %**	**Mo %**	**Ni %**	**Cu %**	**Fe %**
1	0.5840	0.9630	0.9500	0.0870	0.0560	0.0320	0.0050	0.0180	0.0360	97.0800
2	0.5650	0.9200	0.9320	0.0810	0.0410	0.0320	0.0043	0.0200	0.0350	97.1900
3	0.5660	0.9020	0.9280	0.0770	0.0350	0.0330	0.0060	0.0220	0.0370	97.2000
4	0.5630	0.9040	0.9380	0.0720	0.0380	0.0310	0.0042	0.0220	0.0360	97.2100
5	0.5600	0.9410	0.9180	0.0730	0.0340	0.0290	0.0039	0.0180	0.0370	97.2100
Ø	**0.5680**	**0.9260**	**0.9330**	**0.0780**	**0.0410**	**0.0310**	**0.0047**	**0.0200**	**0.0360**	**97.1800**

Ø:Average

Figure 7 shows the optical micrograph of the sample etched with Nital at different magnifications. Figure 8 shows the sample etched with picral. The metallography reveals the formation of martensite obtained by the rapid cooling of austenite. This is a mixture of lath and plate morphologies with a typical formation of medium-carbon steels [20]. Martensite is a single-phase metastable state. In steel, martensite is a tetragonal crystal structure that occurs when steel is rapidly cooled from the austenite phase [21].

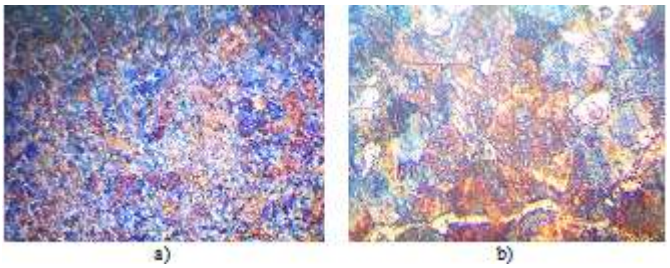

Figure 7. Metallography of the sample etched with Nital at different magnifications: a) 100X, b) 400X

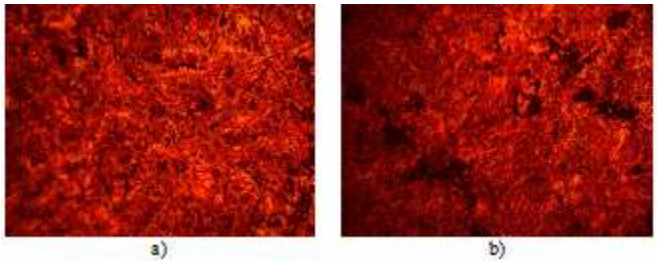

Figure 8. Metallography of the sample etched with Picral at different magnifications: a) 50X, b) 400X.

Figure 9 shows the SEM micrograph using EDS. Chemical elements are present in the section analyzed. Also, non-metallic inclusions are present, particularly hard and non-deformable inclusions.

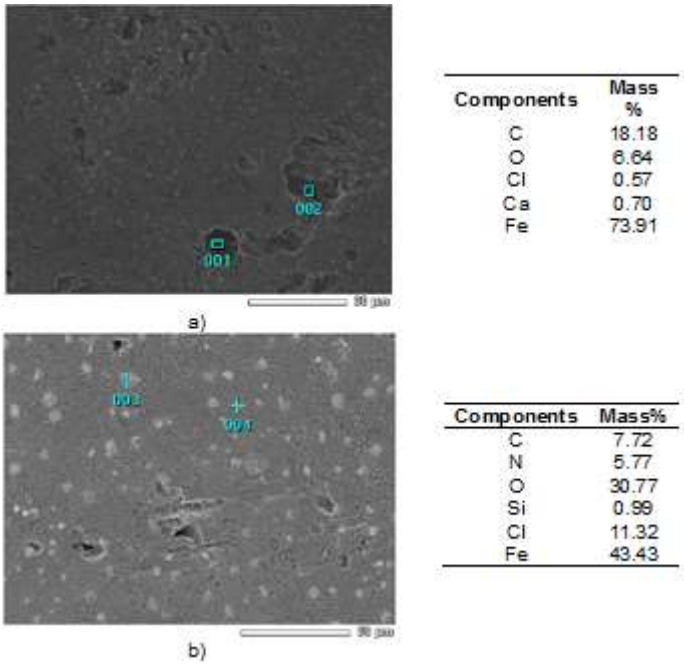

Components	Mass %
C	18.18
O	6.64
Cl	0.57
Ca	0.70
Fe	73.91

Components	Mass%
C	7.72
N	5.77
O	30.77
Si	0.99
Cl	11.32
Fe	43.43

Figure 9. Scanning Electron Microscopy (SEM/EDS): a) Sample etched with Nital, b) Sample etched with Picral.

Figure 10 corresponds to the SEM images of the sample that was chemically etched with Nital. Figure 11shows the sample that was chemically etched with Picral. The micrographs show a matrix with certain porosity that shows irregularities and voids, as well as separation and precipitation of carbides at the grain boundary.

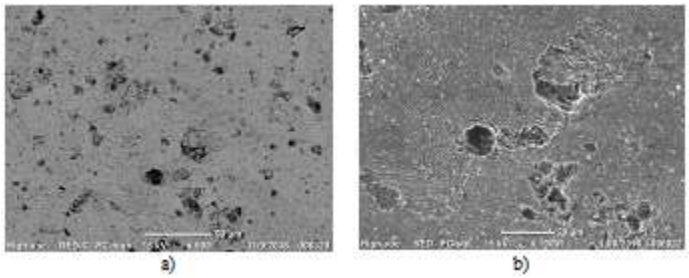

Figure 10. Scanning Electron Microscopy (SEM), Sample etched with Nital: a) zoom 500X, b) Zoom 1000X.

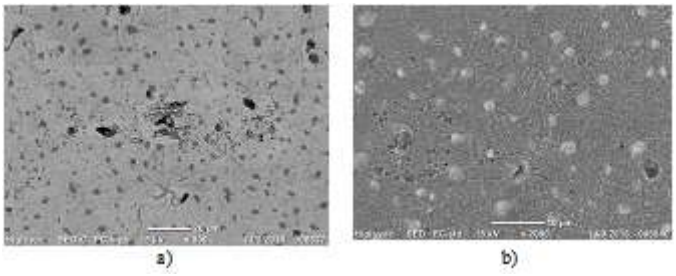

Figure 11. Scanning Electron Microscopy (SEM), Sample etched with Picral: a) 800X b) 2000X.

3.3. Finite Element Analysis (FEA)–

With the drawing of the piece in the computer-aided design (CAD) software, the behavior of the piece was modeled using finite element analysis. ANSYS finite element analysis software was used to simulate the behavior of the part when the machine operates at its maximum capacity of 600kN. The failure occurred in one of the jaws. For the analysis, the load was distributed uniformly, that is, a load of 300 kN was applied. Using the online database MatWeb with the percentages of components described in table 1, an AISI 1040 water quenched steel was selected [22], with the characteristics described in Tables 3 and 4.

Table -3 Chemical composition of AISI 1040 water quenched steel (MatWeb)

Components	%
Carbon, C	0.37 – 0.44
Iron, Fe	98.6 – 99
Manganese, Mn	0.60 – 0.90

Table -4 Mechanical properties of AISI 1040 water quenched steel (MatWeb)

Mechanical properties	Metric system
Hardness, Brinell	223
Hardness, Rockwell B	96
Hardness, Rockwell C	18

Figure 12 shows the simulation for the applied load using AISI 1040 water quenched steel. The modeling shows the maximum deformation and stress supported by the part. When observing the location where the highest stress concentration occurs in the simulation, detailed in red, it is verified that it is the same area where the failure occurred, as shown in Figures 5 and 6.

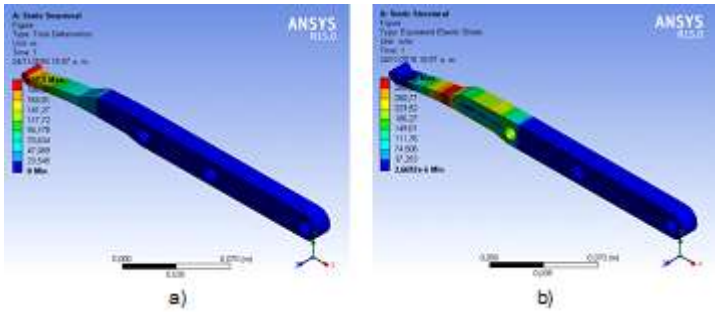

Figure 12. Finite Element Method for the material proposed, AISI 1040 Stainless Steel. a) Maximum deformation, b) Maximum stress.

3.4. Root Cause Failure Analysis–

Visual inspection of the cleavage plane shows that, along the grains, there is high reflectivity with a bright appearance, clearly observable to the naked eye. This is characteristic of a cleavage failure (see Figure 6). The small irregularities and voids observed in the micrographs show the cleavage fracture without plastic deformation. Through the inspection, it was possible to observe that the piece was subjected to metal-to-metal contact between the jaws and the samples used in the tests. The effect of friction and the presence of air subjected the piece to a constant process of oxidation, causing the detachment of material.

During the quenching, the material did not create a homogeneous martensitic surface layer, nor did it create well-defined iron carbides. The carbides precipitated at the grain boundary, and non-metallic inclusions were generated, probably by slower cooling. The finite element analysis showed that the material suffered a plastic deformation of 0.3 %, evidencing fatigue. The precipitation of carbides at the grain boundary and the inclusion of non-deformable, non-metallic elements, as well as the high content of metals such as manganese with body-centered crystal structure, accelerated the fatigue failure. The failure occurred with little plastic deformation, long before the plastic limit of the material was reached, causing the fracture before the matrix completed its plastic deformation.

3.5. Solution–

Following the methodology described in Figure 1, all relevant aspects found were considered as factors that influenced the failure. To prevent future failures, it is necessary to manufacture the part with the appropriate material. The material should be purchased from a certified supplier who guarantees the effectiveness of the heat treatment. To avoid oxidation caused by the contact between the jaw and the sample during the tests, it is proposed to use AISI 304 cold-drawn stainless steel for manufacturing the clamping part of the universal testing machine. The material proposed has the specific properties presented in Tables 5 and 6 [23].

Table -5 Chemical composition of AISI 304 cold-drawn steel (MatWeb)

Components	**%**
Carbon, C	0.07 – 0.08
Iron, Fe	72.40– 75.00
Manganese, Mn	2.00
Chrome, Cr	17.50 – 19.50
Nickel, Ni	8.00 – 10.50

Table -6 Mechanical properties of AISI 304 cold-drawn steel (MatWeb)

Mechanical Properties	
Hardness, Brinell	275
Hardness, Rockwell B	104
Hardness, Rockwell C	28

The material proposed was simulated by the finite element method in ANSYS, as shown in Figure 13. The piece supports the loads with deformations that remain in the elastic limit, with a maximum plastic deformation of 0.00021%.

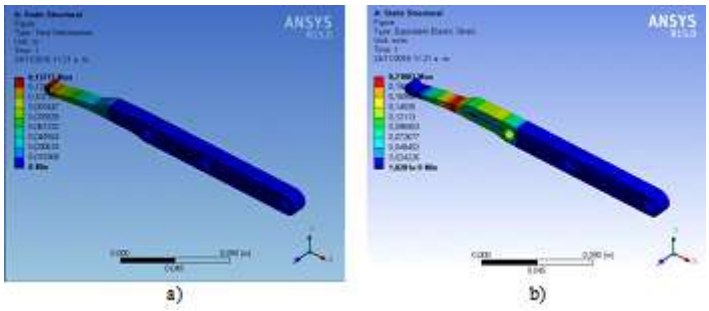

Figure 13. Finite Element Method for the material proposed, AISI 304 Stainless Steel. a) Maximum deformation, b) Maximum stress.

IV.CONCLUSION

The methodology proposed in Figure 1, allowed to systemically analyze the root cause of the failure presented by the fracture of one of the jaws of the universal testing machine model PU-300M. The process carried out in the visual inspection stage made it possible to establish characteristics of the failure presented.

In the second stage of the process, destructive testing allowed an understanding of the hardness, composition, and microstructure of the material. The material studied has an average hardness of 20.86 Rockwell C, practically homogeneous on the surface of the part. Arc/spark optical emission spectrometry revealed that the material has an average carbon content of 0.568%. The material has high concentrations of Silicon Si (0.9260%), which forms a hard, slightly deformable non-metallic inclusion, and Manganese (0.933%), with a body-centered crystal structure, making it less ductile. Metallography indicated the formation of martensite by the transformation of austenite in the quenching process of the medium-carbon steel. The results of the SEM with EDS allowed observing the presence of elements such as silica (Si), and manganese (Mn), as hard and non-deformable inclusions, which due to their crystal structure decrease the number of sliding systems and affect the ductility of the material. There was evidence of grain boundary segregation, and the presence of irregularities, cracks, and voids, indicating a cleavage fracture.

The simulation of the material proposed shows that the deformation decreases from 0.3% to 0.00021%. This ensures that the deformation in the new material will remain within the elastic limit, reducing fatigue.

REFERENCES

[1] K. Silaipillayarputhur, "Maintenace Engineering in Process Plants", EDP Sciences : s.n., International Conference on Mechanics and Mechatronics Research (ICMMR 2016). pp. 1-4, 2016.

[2] J. Moubray, "Reliability-centered maintenance (RCM II)," The Aladon Network, OxfordButterworth-Heinemann1997.

[3] R.K Mobley, "*Root Cause Failure Analysis*". Oxford : Butterworth-Heinemann, 1999.

[4] William. Andrew, "Anticorrosive Rubber Lining: A Practical Guide for Plastics Engineers", Aplied Science Publishers, Elsevier., Oxford, 2017.

[5] P. Ortiz, A. Prado, R. Schouwenaars, E, Ramírez, "Análisis de falla de un semieje", *Ingeniería Mecánica. Tecnología y Desarrollo*, Vol. 2, pp. 22-31, 2005.

[6] E. Ossa, M. Paniagua, "Análisis de falla en cable de acero ", *Ingeniería y Ciencia*, Vol. 1, pp. 97-103, 2005.

[7] W. Lucjan, M. Sikora, F. Stachowicz, T. Trzepiecinski, "Stress and failure analysis of the crankshaft of diesel engine", *Engineering Failure Analysis*. Volume. 82, pp. 703-712, December. 2017.

[8] H. Shabani, N. Goudarzi, M. Shabani, "Failure analysis of a natural gas pipeline", *Engineering Failure Analysis*, Volume. 84, pp. 167-184, February. 2018.

[9] A. Pelliccione, P. Coelho, D. Lopes, C. Ennes, H. Jambo, R. Santanna, "Failure analysis of a stainless steel socket-welding flange due to improper manufacturing process and chemical composition", *Engineering Failure Analysis*, Volume. 108, 104288, January. 2020.

[10] Y. Songa, S. Zengab, J. Ma, J. Houc, "Failure Analysis of Graphite Stationary Ring Utilized in One Type of Mechanical Seal," *Engineering Failure Analysis*, Volume. 108, 104259, January. 2020.

[11] C. Akintoye, R. Tolulope, "Failure Analysis of Metallic Materials: Morphological Characteristics, Mechanisms and Laboratory Investigation", *Journal of Bio- and Tribo-Corrosion*., Volume. 57, 2020.

[12] Lei. Xiaocong, Tongxin. Yu, Baoying. Xing, "Failure modes of mechanical clinching in metal sheet materials.", *Thin-Walled Structures*, Volume. 144, 106281, November. 2019.

[13] H. Zengliang, L. Junting, J. Yongbo, W. Wei, L. Lei, "Failure analysis of corrugated metal hose under ultimate repeated bending process", *Engineering Failure Analysis*, Volume. 109, 104295, January. 2020.

[14] J. Marteau, S. Bouvier, "Characterization of the microstructure evolution and subsurface hardness of graded stainless steel produced by different mechanical or thermochemical surface treatments", Surface and Coatings Technology, pp. 136-148. 2016.

[15] J. Long, A. Borissova, A. D. Wilson, J. C. Avelar, "Sample preparation of anodised aluminium oxide coatings for scanning electron microscopy", *Micron*, Volume. 101, pp. 87-94, October. 2017.

[16] H. P. Jagtap, A. K. Bewoor, R. Kumar, "Failure analysis of induced draft fan used in a thermal power plant using coordinated condition monitoring approach: A case study", *Engineering Failure Analysis*, Volume. 111, 104442, April. 2020.

[17] J. Arana, J. Gonzalés, "Mecánica de Fractura. Bilbao", *Universidad del País Vasco*; Edición. 1, 2002, ISBN-13- 978-8483734551.

[18] L. Johnson, S.R. Fletcher, W. Baker, R.L. Charles,"How and why we need to capture tacit knowledge in manufacturing: Case studies of visual inspection", *Applied Ergonomics*, pp. 1-9, 2019.

[19] Y. Gong, Q. Ding, Z. G. Yang, "Failure analysis on premature fracture of anchor bolts in seawater booster pump of nuclear power plant", *Engineering Failure Analysis*, Volume. 97, pp. 10-19, March. 2019.

[20] T. Toshihiro, I. Kurato, H. Katsutoshi, A. Daichi, N. Nobu, T. Setsuo, K. Tamotsu,"Comparison of Microstructure and Hardness between High-carbon and High-nitrogen Martensites", *Iron and Steel Institute of Japan Journal*, pp. 161-168, 2019.

[21] ASM International. *ASM HANDBOOK Metallography and Microstructures.* s.l. : ASM International, 2004.

[22] MatWeb Material Property Data. [Online] [Cited: April 5, 2019.] http://www.matweb.com/.

[23] MatWeb-Material Property Data. MatWeb-Material Property Data. [Online] [Cited: 10 06, 2017.] http://www.matweb.com/search/DataSheet.aspx?MatGUID=1f1e8f8cff784e08a85ee4eb26968a65&ckck=1